

# Vibration and Friction Damping Analysis of Blades with Dovetail Attachment

Jiao Wang\*, Tao Yu\*\*, Yue-hao Zhang\*\*\* and Qing-kai Han\*\*\*\*

**Keywords** : compressor blade, friction damping, resonant response, normal contact stiffness, normal contact damping

## ABSTRACT

A theoretical method is presented to study the friction damping and contact characteristics of the blade with dovetail attachment. The vibration equation of a cantilever blade considering the friction damping is established, and the response of the blade is calculated by the Galerkin method. The spring and viscous damper are used to describe normal pressure in blade dovetail attachment structure. A cantilever blade is simplified based on natural frequency of the real blade test, and cantilever beam size is obtained. The effects of various parameters including normal contact stiffness, normal contact damping between contact faces of blade dovetail attachment, and rotating angular velocity on dynamic characteristics of blade are studied. The results show that friction damping of blade dovetail attachment can decrease resonance response of the blade. When the normal contact stiffness is maintained at  $10^7$  N/m to  $10^8$  N/m, damping effect is obvious.

## INTRODUCTION

The blade is the key component of aero-engine. At present, the design and manufacture of the blade have reached a high level, and low-cycle fatigue failure or possible flutter failure caused by low-order resonance can be avoided basically. However, blades are subjected to complex loads, including centrifugal force, pneumatic force so that the vibration of the blades is inevitable, and the high-cycle fatigue failure of the blades caused by the high vibration stress level is the most urgent and practical problem.

*Paper Received October 2017. Revised March 2018. Accepted April, 2018. Author for Correspondence: Jiao Wang.*

*\*Associate Professor, School of Mechatronics and Automobile Engineering, Yantai University, Yantai 264005, China.*

*\*\* Professor, School of Mechatronics and Automobile Engineering, Yantai University, Yantai 264005, China*

*\*\*\*Laboratory Technician, Engineering Training Center, Yantai 264005, China*

*\*\*\*\*Professor, School of Mechanical Engineering, Dalian University of Technology, Dalian 116024, China*

Therefore, Voldich et al. (2014) used friction damping at blade-root interfaces to reduce the vibration and the fatigue damage of the blade.

In order to accurately describe the mechanical characteristics of the friction contact surface, many scholars have carried out research on the friction damping model. Den Hartog et al.(1931) first used the Coulomb model to study the structure dynamics behavior, and obtained the accurate solution of the steady state motion of the single degree of freedom oscillator. Gordon(1966)and Pierreet et al.(1985) applied this method in two degrees of freedom system. Muszynska et al.(1982)and Ferri(1988) applied this method in multi degree of freedom system. For the characterization of the sliding state of the dry friction contact surface, there are two mathematical models of macro-slip and micro-slip, which are used to describe the friction mechanism of the contact surface according to the deformation distribution in the contact surface. Macro-slip model can be described by the state of a contact point. It is assumed that the force and deformation of the points in the contact area are evenly distributed in each direction. That is, the normal force and contact stiffness of each contact point are the same. Under the action of the force will produce the same elastic deformation. As the macro-slip model is easy to calculate, it is widely used in the solution of structural dynamic response. Many scholars have studied the dry friction damping structure based on the macro-slip model. By using Coulomb friction law and macroscopic slip model, Yang et al.(1998) studied the transition between viscous friction, slip and other states of dry friction interface of wedge damper, and mathematical description of dry friction force. Chen et al.(2001) studied the periodic response of a blade with a macro-slip model. It is pointed out that the periodic response of the blade exhibits a jump phenomenon due to the nonlinear effect of the dry friction force. Xu et al.(1998)used the macro slip hysteresis model to calculate the vibration response of blades. Hoffmann et al. (2017) presented a new contact model to calculate the forced response of the blade with friction damping, and results agree with the forced response with Coulomb Friction model.

Because of the highly nonlinear friction force at the friction interface, the blade is highly nonlinear, and Chen et al.(2000)obtained analytical solutions of only

a few simple models. For a vibration period in a complex nonlinear contact motion, the contact surface may exist in viscous and sliding. Analytical method cannot be applied to the complex contact motion. At this time, the vibration response of dry friction damping system can only rely on numerical solution. Numerical solution mainly includes time domain method and frequency domain method. The time domain method, including the Newmark method, willson- $\theta$  and Runge-kutta method, and the frequency domain method mainly has harmonic balance method. Krack et al.(2017) gave a comprehensive overview of the method of vibration prediction, the contact model modeling and the numerical simulation of bladed disk with friction damping. Tang et al.(2017) solved the dynamic equations of the mistuned blisk with friction ring damper by using a hybrid frequency/time domain (HFT) method, and used the stick-slip model to describe the contact surface. Lassalle et al.(2018) used HBM method to studied the effect of friction coefficient and normal force on the vibration response of the bladed disk with friction at the blade root. For the results of the response, the numerical simulation is consistent with the experiment. Chen et al.(2000)used the harmonic balance method to study the forced vibration response of a system with three directions of friction constraints, and described resonance, superharmonic resonance and the jump phenomena of the periodic solution caused by the variation of the frequency of the exciting force. Fan(2006)used the macro slip hysteresis model to describe the dry friction force, and established the single degree of freedom and two degrees of freedom mechanics model with dry friction damper system. The Fourier series expansion method, the incremental harmonic balance method and the fine integration method are used to solve the model respectively. The results of the incremental harmonic balance method are slightly smaller but convergent stronger, the calculation process is less dependent on the initial value, and the results of the fine integration method is basically consistent but the workload should be significantly reduced. Papanikos et al.(1995) used the incremental harmonic balance method and the precise integration method to solve the response of the single degree of freedom dry friction damping system model. Compared with the results of the fourth-order Runger-Kutta numerical integration method, the results are in good agreement. Bottoet al.(2015) proposed a new method to solve the contact problem of elastic bodied based on FEM. This method is not restricted to special geometries and anisotropic materials, which is convenient to be applied in wear simulation. Sazhenkova et al.(2017) presented a numerical method to study the blade with underplatform friction damper. Considering the effect of friction factor on the resonant amplitudes of the blade. The results show that the existence of optimal friction coefficient can reduce the resonant amplitude

of the blade. Afzal et al.(2018) studied the effect of the multiple friction contacts(a strip damper and shroud contact) on the nonlinear response of bladed disks. The results show that multiple friction contacts compared with single friction can effectively reduce the vibration of the bladed disks.

In addition, domestic and foreign scholars have done a lot of research on the fatigue test of dovetail attachment structure. Papanikos et al. used the photoelasticity test technique to obtain the stress results of the blade-root contact area, and verified the simulation results. The results show that this technique can effectively observe the structure of most of the region. Rajasekaran et al.(2006) carried out the fatigue test on dovetail attachment structure, and used the semi-analytical method to accurately estimate the surface external force and internal stress of the finite element model of dovetail attachment structure. The method was applied to the analysis of the two-axis fatigue test, and the boundary conditions of centrifugal load, disk expansion force and blade vibration are also simulated accurately. The results show that the high friction coefficient is more likely to lead to the occurrence of the fault. Araujoetal(2009)studied the effect of complex contact loads on fretting fatigue by fatigue tests. The results show that the influence of fretting fatigue life is mainly related to the size of tangential force and the residual stress due to shot peening. Xia(2005) used fretting fatigue test to study on dovetail attachment structure under three kinds of loads, and the fretting fatigue life of the dovetail attachment structure under low cycle load was predicted. The comparison between the predicted results and the experimental results verifies the effectiveness of the prediction method. Yang et al. (2007), Gu et al.(2007) and Wang et al.(2008) studied the fatigue reliability test of the dovetail structure and established the fatigue life prediction model. The correctness of the established reliability model was verified by comparison with the experimental data. Pesaresi et al.(2017)designed an underplatform damper test rig to study the nonlinear characteristics of the blades.

However, the traditional dry friction damping theory has little research on the influence of the contact force on the vibration characteristics of blade, and the contact normal force is often treated as a constant value. In addition, there are few experimental studies on the influence of the contact characteristics on the vibration characteristics of the blade, and the test is mostly fatigue test. In this paper, the simplified mechanical model of blade with dovetail attachment is established. The viscous dampers and the coulomb friction model are used to describe the normal pressure and the dry friction between dovetail attachment of the blade. The motion equation of the blade considering friction damping is established and Galerkin method is used to obtain three degree of freedom contact friction model in order to calculate natural frequency and

response of the blade. The effects of normal contact stiffness, normal contact damping at blade-root interfaces, and rotating speed on dynamic characteristics of blade are discussed in detail. The results show that the friction damping can decrease resonant response of the blade, and the measured results verify the rationality of the simulation results.

## THEORETICAL ANALYSIS

### Mechanical model of the blade

Bladed disc of an aeroengine is composed of blades and disc, as shown in Fig.1(a). The overall coordinate system  $OXYZ$  is set up on the bladed disc, and point  $O$  is located in the center of the disc. The disc is rotated at the angular velocity of  $\Omega$ . The local coordinate system  $oxyz$  is set up on the blade, and point  $o$  is at the bottom of the blade root. The size of  $R$  is  $Oo$ .

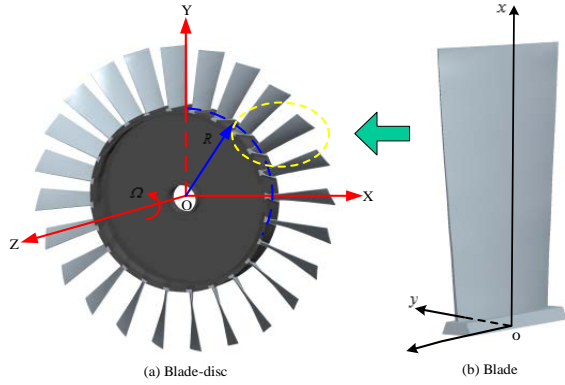


Fig.1 Sketch map of the bladed disc considering friction damping at the blade root

Blade is simplified as a cantilever beam, as shown in Figure2. The density, elasticity modulus and Poisson's ratio of the blade materials are denoted by  $\rho$ ,  $E$ , and  $\nu$ , respectively. Length, width, thickness and cross-sectional area cantilever beam are represented by  $L_0$ ,  $B$ ,  $H$ , and  $A$ . The force and deformation of a simplified cantilever beam are defined in a local coordinate system  $oxyz$ . As shown in Fig. 2, the displacement along the  $x$ ,  $y$  and  $z$  directions of the blade are  $u(x,t)$ ,  $v(x,t)$  and  $w(x,t)$ , respectively. The loads acting on the blade have the pneumatic load  $F_a(t)$ , the positive pressure  $F_N$ , the friction force  $F_f$  and friction factor  $\mu$  the contact surface of blade-root.

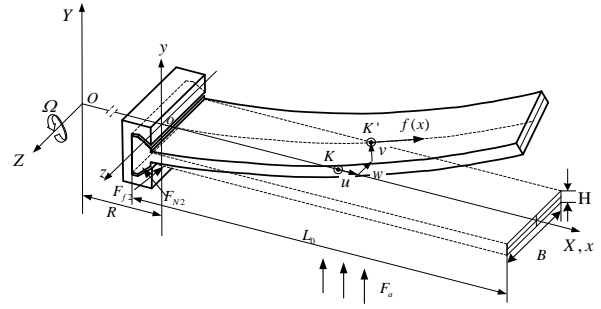


Fig.2. Sketch map of a cantilever beam considering friction damping at the blade root

The spring and viscous dampers are used to describe the normal pressure  $F_{N1}$  and  $F_{N2}$  between dovetail attachment of the blade, and the coulomb friction model are used to describe the dry friction  $F_{f1}$  and  $F_{f2}$  between dovetail attachment of the blade, as shown in Fig.3. Blade-root and disc-slot is always contact, and the normal direction does not change (Zhang et al, 2001).

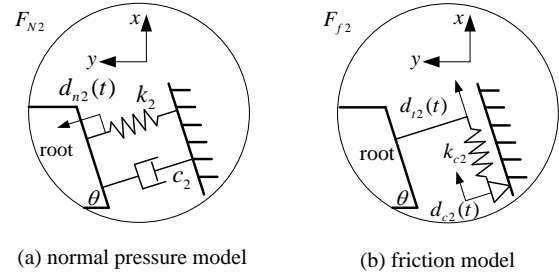


Fig. 3 Contact force model at the blade root

Bottom angle of the dovetail is  $\theta$ , the lateral displacement of the blade is  $v(x,t)$ . The normal pressure applied to the blade-root can be expressed as

$$F_{N1} = k_1 v_c \sin \theta + c_1 \dot{v}_c \sin \theta, \quad (1)$$

$$F_{N2} = -k_2 v_c \sin \theta - c_2 \dot{v}_c \sin \theta, \quad (2)$$

where,  $v_c = v(L_c, t)$  is the displacement of the contact force,  $L_c$  is the distance from origin to contact force.

Friction between dovetail attachment is

$$F_{f1} = \mu F_{N1} \operatorname{sgn}(\dot{v}_c), \quad (3)$$

$$F_{f2} = \mu F_{N2} \operatorname{sgn}(\dot{v}_c), \quad (4)$$

Force in the  $y$  direction to do decomposition, we have

$$F_{Ny} = -F_{N1} \sin \theta + F_{N2} \sin \theta = \sin^2 \theta [(-k_1 - k_2)v_c + (-c_1 - c_2)\dot{v}_c], \quad (5)$$

$$F_{fy} = -F_{f1} \cos \theta - F_{f2} \cos \theta = \mu \sin \theta \cos \theta \operatorname{sgn}(\dot{v}_c) [(-k_1 + k_2)v_c + (-c_1 + c_2)\dot{v}_c], \quad (6)$$

The contact force generated by lateral vibration of the blade is

$$F_{cy} = F_{Ny} + F_{fy}$$

$$= \left[ \mu \sin \theta \cos \theta \operatorname{sgn}(\dot{v}_c) - \sin^2 \theta \right] (k_2 v_c + c_2 \dot{v}_c) \quad (7)$$

$$- \left[ \mu \sin \theta \cos \theta \operatorname{sgn}(\dot{v}_c) + \sin^2 \theta \right] (k_1 v_c + c_1 \dot{v}_c)$$

**Governing equations of the blade with contact friction**

The Newton mechanics method is used to build the governing equation of the blade considering contact friction. In order to setup an effective kinetic model of the blade-root contact friction, the following assumptions are used(Cui,2008; Kaya,2006).

- 1)The blade with dovetail attachment is simplified to cantilever beam and the lateral vibration of the cantilever beam is micro vibration.
- 2)The geometric parameters of all cross sections of the blade remain unchanged in the plane.
- 3)Based on the assumption of Euler-Bernoulli beam, the cross-section of the cantilever beam always perpendicular to the neutral axis before and after deformation. The shear, torsion and warping effects are ignored.
- 4)The influence of damping of the material on the vibration is not considered.
- 5)The Coriolis effect is not considered. Neglecting the longitudinal displacement  $u$  of the cantilever beam and the displacement  $w$  along the direction of the shaft. Inspect a point  $K$  on the center axis of the beam element  $dx$ , and it moves to the point  $K'$  after deformation, as shown in Fig 2.

The location vector  $r_o$  of the micro-body  $dx$  in  $OXYZ$  is represented as

$$r_o = (R+x)\mathbf{i} + v(x,t)\mathbf{j} \quad (8)$$

where  $\mathbf{i}, \mathbf{j}$  are the unit vectors along the blade axis  $OX, OY$ , and  $\mathbf{i} = \mathbf{i}', \mathbf{j} = \mathbf{j}'$ .

The inertial velocity vector and acceleration vector of the micro-body  $dx$  can be represented as

$$v_a = v_x \mathbf{i} + v_y \mathbf{j}$$

$$a_a = a_x \mathbf{i} + a_y \mathbf{j} \quad (9)$$

in which

$$\begin{cases} v_x = -v(x,t)\Omega \\ v_y = (R+x)\Omega + \frac{\partial v(x,t)}{\partial t} \end{cases} \quad (10)$$

$$\begin{cases} a_x = -\Omega^2(R+x) - 2\Omega \frac{\partial v(x,t)}{\partial t} \\ a_y = \frac{\partial v^2(x,t)}{\partial t^2} - \Omega^2 v \end{cases} \quad (11)$$

According to the principle of Newton mechanics, the motion governing equations of the blade with dovetail attachment are built. The blade with dovetail attachment is simplified as a cantilever beam, take one micro-body  $dx$  at  $x$  position on it.

The mechanical analysis is shown in Fig. 4.

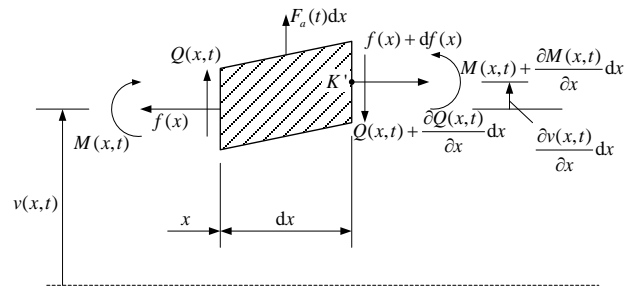


Fig.4 Mechanical schematics of blade microelement

Based on the hypothesis, the lateral vibration of the blade is considered only. Therefore, considering the force balance of  $y$  direction, the contact friction force is introduced, and the relation between the lateral vibration displacement and the lateral forces is obtained.

$$Q(x,t) - \left[ Q(x,t) + \frac{\partial Q(x,t)}{\partial x} dx \right] + F_a(t)dx + F_{cy} D(x-L_c)dx = \rho A dx a_y \quad (12)$$

where  $Q(x,t)$  is the shear force, corresponding deformation is  $\frac{\partial Q(x,t)}{\partial x} dx$ ,  $F_a(t)$  is the pneumatic load caused by the wake vibration of the former stator blades.

$$F_a(t) = F_{a0} \cos(jN\Omega t) \quad , j = 1, 2, 3, \dots \quad (13)$$

where  $F_{a0}$  is amplitude of  $F_a(t)$ ,  $j$  is the resonant order,  $N$  is the upstream blade row number,  $\Omega$  is the rotational angular velocity.

$D(x-L_c)$  is a Dirac function that satisfies

$$D(x) = \begin{cases} +\infty, & x = 0 \\ 0, & x \neq 0 \end{cases} \text{ and } \int_{-\infty}^{+\infty} D(x)dx = 1$$

Substitute  $a_y = \frac{\partial v^2(x,t)}{\partial t^2} - \Omega^2 v$  into Eq.(12)

and divide it by  $dx$

$$\frac{\partial Q(x,t)}{\partial x} = -\rho A \frac{\partial v^2(x,t)}{\partial t^2} + \rho A \Omega^2 v + F_a(t) + F_{cy} D(x-L_c) \quad (14)$$

The rotation equation of the micro-element is obtained by taking the moment balance of the  $K'$  point of the micro - element

$$\left( M(x,t) + \frac{\partial M(x,t)}{\partial x} dx \right) - M(x,t) - Q(x,t)dx - f(x) \frac{\partial v(x,t)}{\partial t} dx - F_a(t)dx \frac{dx}{2} = 0 \quad (15)$$

where,  $f(x)$  is the axial centrifugal load

$$f(x) = \int_x^L \rho A \Omega^2 (R+x) dx = -\frac{1}{2} \rho A \Omega^2 (x-L)(x+2R+L) \quad (16)$$

Omit  $(dx)^2$ , and simplify Eq. (15) to

$$Q(x,t) = \frac{\partial M(x,t)}{\partial x} - f(x) \frac{\partial v(x,t)}{\partial x}, \quad (17)$$

Based on the assumption 1), in the case of small deformation, bending moment and deflection have the following relationship

$$M(x,t) = EI \frac{\partial^2 v(x,t)}{\partial x^2}, \quad (18)$$

By substituting Eq. (17) and Eq. (18) into Eq. (14), the differential equation of transverse vibration of blade considering the contact friction is obtained.

$$\begin{aligned} EI \frac{\partial^4 v(x,t)}{\partial x^4} + \rho A \frac{\partial^2 v(x,t)}{\partial t^2} \\ + \frac{1}{2} \rho A \Omega^2 (x-L)(x+2R+L) \frac{\partial^2 v(x,t)}{\partial x^2}, \quad (19) \\ + \rho A \Omega^2 (x+R) \frac{\partial v(x,t)}{\partial x} - \rho A \Omega^2 v(x,t) \\ - F_{cy} D(x-L_c) = F_a(t) \end{aligned}$$

### SOLUTION OF THE BLADE MOTION EQUATION CONSIDERING CONTACT FRICTION

#### Galerkin Discrete

The dynamic Eq. (19) of the blade considering contact friction is discretized by Galerkin method, and then solved. Under the given cantilever boundary condition, the natural frequency  $\omega_i$  of the blade is set, and the corresponding mode shape function  $\phi_i(x)$  is introduced. The generalized coordinate  $q_i(t)$  is introduced, and the solution of Eq. (19) can be set as

$$v(x,t) = \sum_{i=1}^n \phi_i(x) q_i(t), \quad (20)$$

where,  $n$  is the intercept order, take the first  $n$ -order mode

The eigen-function is

$$\begin{aligned} \phi_i(x) = \cosh \frac{\lambda_i}{L} x - \cos \frac{\lambda_i}{L} x \\ - \frac{\cosh \lambda_i + \cos \lambda_i}{\sinh \lambda_i + \sin \lambda_i} \left( \sinh \frac{\lambda_i}{L} x - \sin \frac{\lambda_i}{L} x \right), \quad (21) \end{aligned}$$

where  $\lambda_i$  is eigenvalues, meets

$\cos(\lambda_i) \cosh(\lambda_i) + 1 = 0$ ,  $L$  is the length of the beam, meets  $L = L_0$ .

According to the orthogonality of the mode

$$\mathbf{K}_e = \frac{EI}{L^3} \text{diag}(\lambda_1^4, \lambda_2^4, \dots, \lambda_n^4)_{n \times n}, \quad (24)$$

$$\begin{aligned} \mathbf{K}_{con} = \left( \mu \sin \theta \cos \theta \text{sgn} \left( \sum_{i=1}^n \phi_i(L_c) \dot{q}_i(t) \right) (k_2 - k_1) - \sin^2 \theta (k_1 + k_2) \right) \\ \text{diag}(\phi_1^2(L_c), \phi_2^2(L_c), \dots, \phi_n^2(L_c))_{n \times n} \end{aligned} \quad (25)$$

$$\text{shape function, } \int_0^L \phi_i(x) \phi_k(x) dx = \begin{cases} 0 & (k \neq i) \\ L & (k = i) \end{cases},$$

$$\int_0^L \phi_i^{(4)}(x) \phi_k(x) dx = \begin{cases} 0 & (k \neq i) \\ \frac{\lambda_i^4}{L^3} & (k = i) \end{cases}, \text{ the equations can}$$

be discretized.

Substituting Eq. (20) into Eq. (19), the equations are multiplied by  $\phi_k(x)$  on both sides, and the integral of  $x$  on the whole interval  $[0, L]$  is obtained.

$$\begin{aligned} EI \sum_{i=1}^n q_i(t) d_1 + \rho A \sum_{i=1}^n \ddot{q}_i(t) d_2 + \frac{1}{2} \rho A \Omega^2 \sum_{i=1}^n q_i(t) d_3 \\ - \rho A \Omega^2 \sum_{i=1}^n q_i(t) d_4 + \rho A \Omega^2 \sum_{i=1}^n q_i(t) d_5 \\ + d_6 \sum_{i=1}^n q_i(t) d_5 + d_7 \sum_{i=1}^n \dot{q}_i(t) d_5 \\ = \int_0^L F_{a0} \phi_k(x) \cos(jN\Omega t) dx, (k = 1, 2, \dots, n) \end{aligned} \quad (22)$$

$$\text{where, } d_1 = \int_0^L \phi_i^{(4)}(x) \phi_k(x) dx, \quad d_2 = \int_0^L \phi_i(x) \phi_k(x) dx$$

$$d_3 = \int_0^L (x-L)(x+2R+L) \phi_i^{(2)}(x) \phi_k(x) dx, \quad d_4 = \int_0^L (x+R)$$

$$\phi_i^{(1)}(x) \phi_k(x) dx, \quad d_5 = \int_0^L \phi_i(L_c) \phi_k(x) D(x-L_c) dx,$$

$$d_6 = \left( \mu \sin \theta \cos \theta \text{sgn} \left( \sum_{i=1}^n \phi_i(L_c) \dot{q}_i(t) \right) (k_2 - k_1) - \sin^2 \theta (k_1 + k_2) \right)$$

$$d_7 = \left( \mu \sin \theta \cos \theta \text{sgn} \left( \sum_{i=1}^n \phi_i(L_c) \dot{q}_i(t) \right) (c_2 - c_1) - \sin^2 \theta (c_1 + c_2) \right)$$

where  $\phi_i^{(m)}(x) = \frac{d^m \phi_i(x)}{dx}$ , means  $m$ -order derivative

of the mode function for  $x$ .

Eq. (22) can be written as follows

$$\mathbf{M} \ddot{\mathbf{q}}(t) + \mathbf{C} \dot{\mathbf{q}}(t) + \mathbf{K} \mathbf{q}(t) = \mathbf{F}(t), \quad (23)$$

where  $\mathbf{q}(t) = \{q_1(t), \dots, q_n(t)\}^T$  is displacement vector,

$\mathbf{M} = \rho A L \text{diag}(1, 1, \dots, 1)_{n \times n}$  is the mass matrix,

$\mathbf{K} = \mathbf{K}_e + \mathbf{K}_c + \mathbf{K}_{con}$  is stiffness matrix of the blade,

with asymmetric characteristics.  $\mathbf{K}_e$ ,  $\mathbf{K}_{con}$  and  $\mathbf{K}_c$  are

the elastic stiffness matrix, the centrifugal stiffness

matrix and contact stiffness matrix, respectively. And

expression is as follows Eq.(24)-Eq.(26).  $\mathbf{C}_{con}$  is the

contact damping matrix, and its expression is as

Eq.(27).  $\mathbf{F}(t)$  is expressed as Eq.(28).

$$\mathbf{K}_c = \frac{1}{2} \rho A \Omega^2 \begin{bmatrix} \int_0^L (x-L)(x+2R+L)\phi_1^{(2)}(x)\phi_1(x)dx & \dots & \int_0^L (x-L)(x+2R+L)\phi_1^{(2)}(x)\phi_n(x)dx \\ \vdots & \ddots & \vdots \\ \int_0^L (x-L)(x+2R+L)\phi_n^{(2)}(x)\phi_1(x)dx & \dots & \int_0^L (x-L)(x+2R+L)\phi_n^{(2)}(x)\phi_n(x)dx \end{bmatrix}_{n \times n} \quad (26)$$

$$+ \rho A \Omega^2 \begin{bmatrix} \int_0^L (x+R)\phi_1^{(1)}(x)\phi_1(x)dx & \dots & \int_0^L (x+R)\phi_1^{(1)}(x)\phi_n(x)dx \\ \vdots & \ddots & \vdots \\ \int_0^L (x+R)\phi_n^{(1)}(x)\phi_1(x)dx & \dots & \int_0^L (x+R)\phi_n^{(1)}(x)\phi_n(x)dx \end{bmatrix}_{n \times n} - \rho A \Omega^2 L \text{diag}(1,1,\dots,1)_{n \times n}$$

In the damping matrix,  $\mathbf{C}_r = \alpha \mathbf{M} + \beta \mathbf{K}_e$  is proportional damping. The proportional coefficient  $\alpha = 2(\xi_2/\omega_2 - \xi_1/\omega_1)/(1/\omega_2^2 - 1/\omega_1^2)$ ,  $\beta = 2(\xi_2\omega_2 - \xi_1\omega_1)/(\omega_2^2 - \omega_1^2)$  can be calculated by measuring modal damping ratio of the blade. Where  $\xi_1, \xi_2$  is first and second order modal damping ratio,  $\omega_1, \omega_2$  is first and second order bending frequency of the blade.

$$\mathbf{C}_{con} = \left( \mu \sin \theta \cos \theta \text{sgn} \left( \sum_{i=1}^n \phi_i(L_c) \dot{q}_i(t) \right) (c_2 - c_1) - \sin^2 \theta (c_1 + c_2) \right) \text{diag}(\phi_1^2(L_c), \phi_2^2(L_c), \dots, \phi_n^2(L_c))_{n \times n} \quad (27)$$

$$\mathbf{F}(t) = F_{a0} \cos(jN\Omega t) \cdot \left[ \int_0^L \phi_1(x)dx, \int_0^L \phi_2(x)dx, \dots, \int_0^L \phi_n(x)dx \right]^T, \quad (28)$$

**Response solution**

The vibration differential Eq.(23) can be solved by numerical method, and the response in the generalized coordinates is transformed into physical coordinates. The frequency domain response in the physical coordinate system is obtained.

$$v(x_0, t) = \sum_{i=1}^n \phi_i(x) q_i(t), \quad (29)$$

where  $x_0$  is the height of the pickup response point from the origin  $o$ , meets  $0 \leq x_0 \leq L$ ,  $x_0 = 0$  at the blade-root,  $x_0 = L$  at the blade tip.

**SIMULATION ANALYSIS AND RESULTS DISCUSSION**

The vibration response of the blade considering friction damping is mainly studied. The effects of contact parameters including normal contact stiffness, normal contact damping and the rotational angular velocity on vibration amplitude are discussed. In the simulation analysis, set the speed of the blade to 0 r/min for comparison with the static test data. According to Eq.(13) and Eq.(23), the other parameters are shown as Table.1. In addition, the influence of the speed on frequency of the blade with contact friction, the rotational speed range is from 0 to

$6 \times 10^4$  rpm. The material (Wang, 2013) and contact parameters of the blade are shown in Table.2 and Table.3. The quality of the blade is 166.6g.

Table.1 The parameters of the simulation analysis

$N$	$j$	$R$	$M$	$K$
36	1	1.2 $L$	3×3	3×3

Table.2 Material parameters of the blade

Material	$E$ /Pa	$V$	$\rho$ / (kg / m <sup>3</sup> )
1Cr11Ni2W2MoV	$214 \times 10^9$	0.3	7800

Table.3 Contact parameters of the blade at the root

Contact stiffness	Contact damping	Friction factor
$1 \times 10^7$	40	0.3

The vibration table is used to test the natural frequency and vibration response of the blade. In order to consider the influence of the blade root friction on the blade dynamics, 10N.m and 50N.m torques are applied to the blade holder, respectively. The natural frequency of the blade is tested by a vibrating table, and then the response of the blade is tested using a fixed-frequency excitation method. The excitation energy is 0.5g to 2.5g. The vibration response of blades is obtained through pickup of laser sensors, and data acquisition is done through LMS acquisition system. The schematic diagram of the experiment is shown in Fig 5. The theoretical analysis mainly uses experimental data obtained with the pretightening torque of 50 N.m, as shown in Table 4. From Table 4, it can be seen that the contact friction has effect on the natural frequency.

Geometric parameters of cantilever beam is obtained according to the testing the first three natural frequency of the real blade. The natural frequency of the beam is calculated as follows

$$\omega_i = \frac{\lambda_i^2}{L^2} \sqrt{\frac{EI}{\rho A}} = \frac{\lambda_i^2 H}{L^2} \sqrt{\frac{E}{12\rho}}, \quad (30)$$

where,  $\omega_i$  is the natural frequency of blade measured by experiment.

The length and width of the cantilever beam are 45.6mm and 130mm, respectively. Then according to Eq. (30) the thickness  $H$  of the first three order cantilever beams is 5.07mm, 3.22mm, and 1.35.

Table.4 Natural frequencies and modal damping ratio of the blade are obtained by experiment

Order	50N.m		10N.m	
	Natural frequency	Damping ratio/%	Natural frequency	Damping ratio/%
1	253.00Hz	0.1617	252.25Hz	0.0987
2	1011.15Hz	0.0812	1008.5Hz	0.0678
3	1189.25Hz	0.0256	1187.5Hz	0.0287

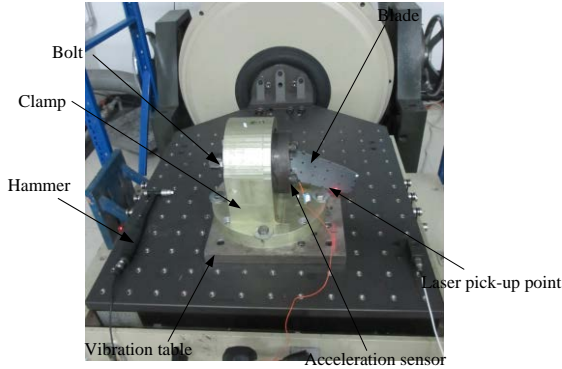


Fig. 5 Schematic diagram of test blade and the fixture

**Response analysis of the blade**

The response of the blade considering the root contact friction in the static state is calculated and compared with the test data. The exciting energy is simulated by uniformly distributed pneumatic load, which changes from 0.5g to 2.5g. Taking the calculation results corresponding to the first three order frequency as an example, the influence of the contact friction on the vibration amplitude of the blade is illustrated. The results are shown in Table.5, 6 and 7. The resonance curve of the blade tip with or without contact friction under different exciting forces is shown in Fig.6.

From the Figures and Tables show that the vibration amplitude of the blade considering contact friction changes as follows:

(1)In the case of the same excitation energy, the first order vibration amplitude of the blade is larger than that of the other order.

(2)Taking the first-order vibration of the blade as an example, the amplitude of the blade considering the friction damping is reduced compared with the blade which does not consider the friction damping. When the excitation energy is 0.5g, the vibration amplitude of the blade is reduced by 0.4%.

(3)The difference between the two cases increases with the increase of excitation energy, which indicates that the greater the excitation energy is, the more obvious the friction damping effect.

Table.5 Comparison of the 1<sup>st</sup> order amplitude of the pure blade(A)and the blade with friction (B)/mm

Excitation energies	0.5g	1g	1.5g	2g	2.5g
A	0.01337	0.0267	0.0802	0.3210	1.6053
B	0.01331	0.0265	0.0791	0.3151	1.5683
A - B /A	0.4%	0.7%	1.3%	1.8%	2.3%

Table.6 Comparison of the 2<sup>nd</sup> order amplitude of the pure blade(A)and the blade with friction (B)/mm

Excitation energies	0.5g	1g	1.5g	2g	2.5g
A	1.8915 430e-5	3.7830 859e-5	0.0001 135	0.0004 539	0.0022 698
B	1.8894 329e-5	3.7746 489e-5	0.0001 131	0.0004 519	0.0022 572
A - B /A	0.1%	0.2%	0.3%	0.004%	0.5%

Table.7 Comparison of the 3<sup>rd</sup> order amplitude of the pure blade(A)and the blade with friction (B)/mm

Excitation energies	0.5g	1g	1.5g	2g	2.5g
A	9.2039 809e-6	1.8407 962e-5	5.5223 890e-5	0.0002 209	0.0011 045
B	9.1561 570e-6	1.8216 590e-5	5.4362 848e-5	0.0002 163	0.0010 759
A - B /A	0.5%	1.0%	1.5%	2.1%	2.5%

Table.8 Comparison of experimental and theoretical simulation results of the blade

Excitation Energy	Simulation results/mm		Test results/mm	
	A	B	10N.m	50N.m
0.5g	0.01337	0.01331	0.3596	0.3586
	A - B /A		A - B /A	
	0.4487		0.2781	

In order to better verify the correctness of numerical simulation, the experimental results are compared with simulation results shown in Table 8. It can be seen that the vibration amplitude of the blade is slightly reduced after considering the friction, and the experimental and simulation results have the same downward trend. but there is an order of magnitude error between simulation and test values. The main reason for the error is that the experiment adopts the basic excitation, while the numerical simulation uses the airflow excitation.

**Influence of contact parameters on blade response characteristics**

The effects of normal contact stiffness, normal contact damping between the contact surfaces on the response characteristics of the blade are investigated. Considering the influence of the above parameters on the response characteristics of blade, the range of the contact parameters is shown in Table.9. Assuming that the normal contact stiffness at the blade-root contact interfaces changes from 10<sup>4</sup> -10<sup>8</sup>N/m .In Table.10 and Fig. 9, the first three order amplitude of the blade varies with the normal contact stiffness.

Table.9 The range of the contact parameters

Contact stiffness /(N/m)	Contact damping /(Ns/m)
10 <sup>4</sup> ~ 10 <sup>8</sup>	10~90

Table.10 Vibration amplitude of the cantilever beam under different contact stiffness/mm

	$10^4$ N/m	$10^5$ N/m	$10^6$ N/m	$10^7$ N/m	$10^8$ N/m
1	0.0133 776	0.0133 770	0.0133 714	0.0133 155	0.0127 832
2	1.891496 4e-5	1.8914778 4e-5	1.891291 8e-5	1.889432 9e-5	1.870961 4e-5
3	9.202365 8e-6	9.2019 504e-6	9.1977 963e-6	9.1561 570e-6	8.7525 658e-6

Table.11 Vibration amplitude of the cantilever beam under different normal contact damping/mm

	10Ns/m	30Ns/m	50Ns/m	70Ns/m	90Ns/m
1	0.013315 561	0.013315 5571	0.013315 553	0.013315 549	0.013315 545
2	1.889466 27e-5	1.889444 04e-5	1.889421 81e-5	1.889399 59e-5	1.889377 36e-5
3	9.157311 42e-6	9.156541 84e-6	9.155772 30e-6	9.155002 80e-6	9.154233 35e-6

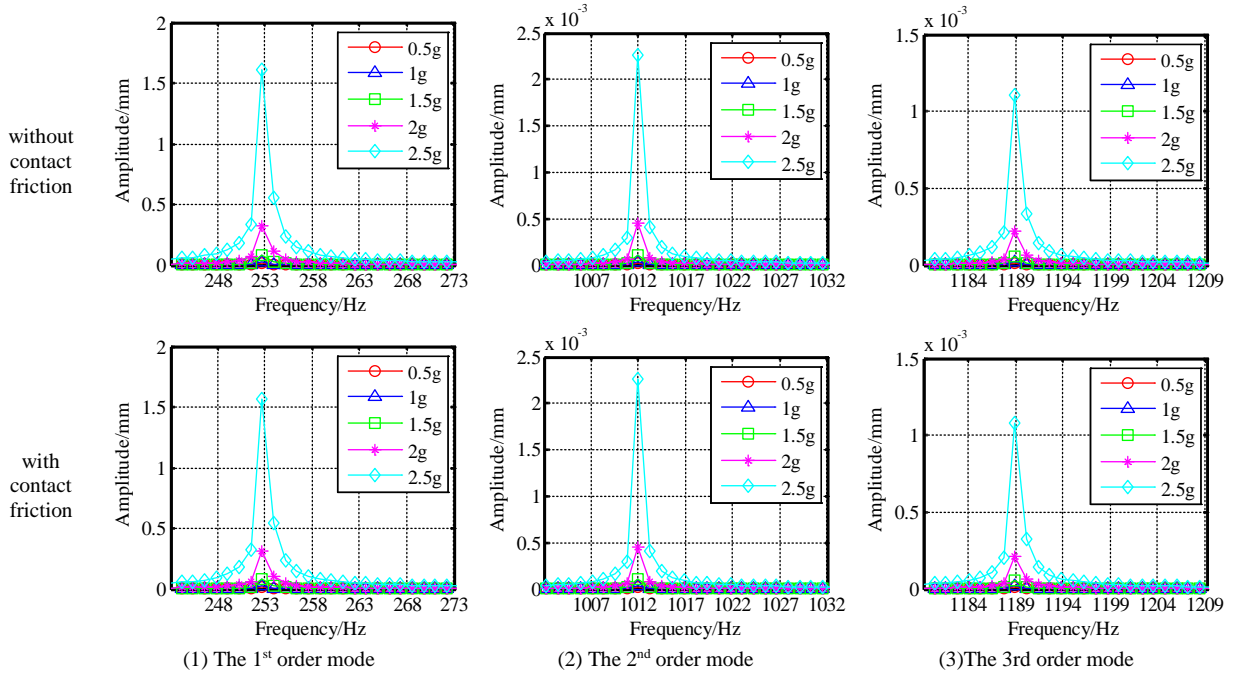


Fig. 6 The first three order amplitude of the blade with and without friction under different excitation energies

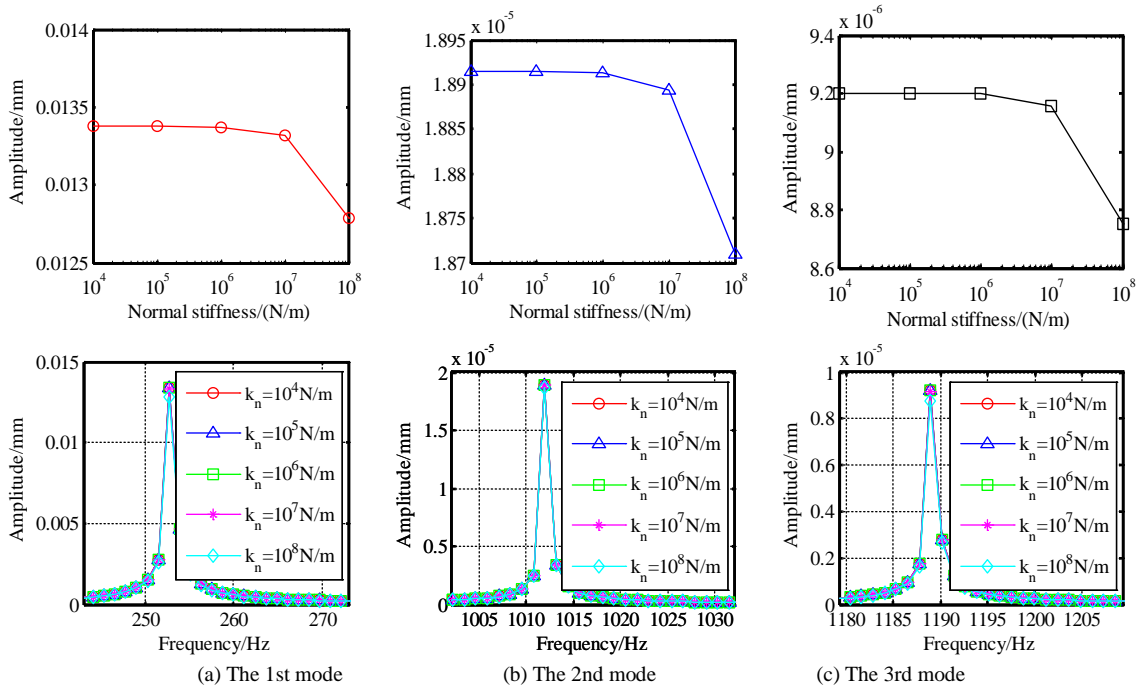


Fig.7 Vibration amplitude of the blade with contact friction under different contact stiffness

It can be seen from Table. 10 and Fig. 7 that the first three resonance response amplitude of blade decreases with the increase of normal contact stiffness. When the normal stiffness of the contact area is above

$10^7\text{N/m}$  to  $10^8\text{N/m}$ , the amplitude of resonant response decreases obviously. Assuming that the contact damping of the blade-root contact interfaces changes from  $10\text{Ns/m}$  to  $90\text{Ns/m}$ . In Table.11 and Fig. 8, the response amplitude of the blade varies with the normal

contact damping. As shown in Table 11 and Fig.8, with the change of normal contact damping in contact interfaces of the blade-root, the first three order vibration amplitude of blade decreases with the increase of blade normal contact damping.

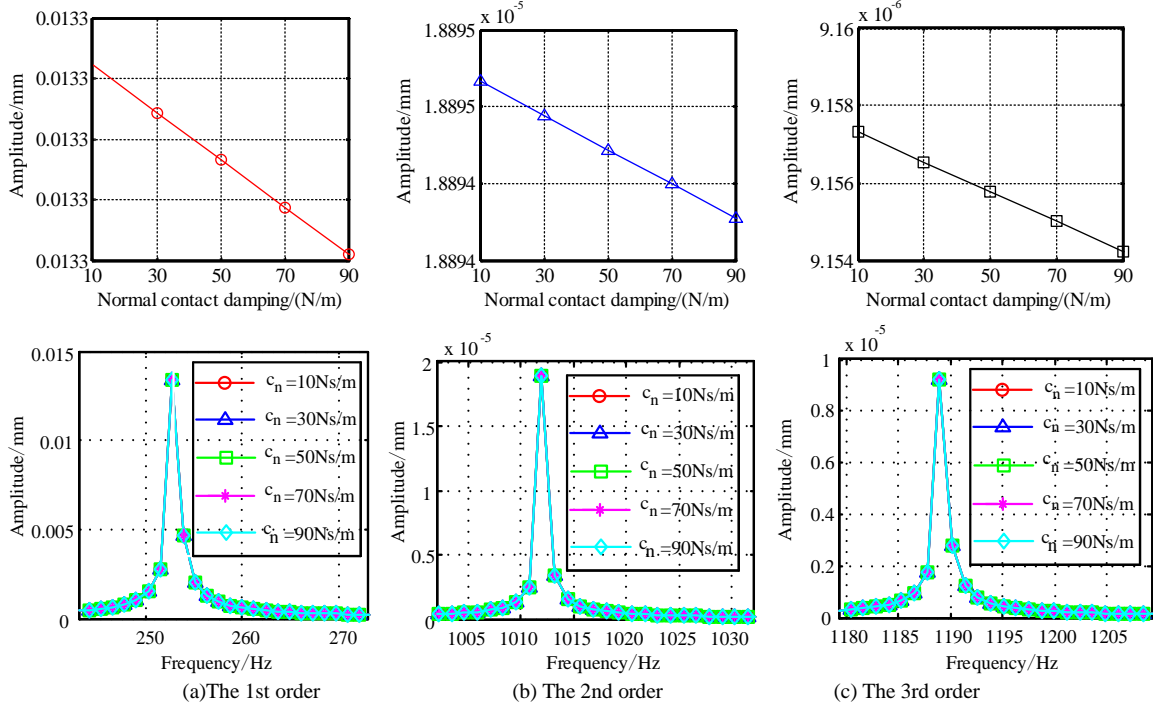


Fig.8 Vibration amplitude of the blade with contact friction under different normal contact damping

### The effect of rotating angular velocity on natural frequency

The natural frequencies of the blade considering the contact friction under different rotating angular velocity conditions are obtained, and the Campbell diagram is drawn as shown in Fig.9. It can be seen from the Fig.11 that when the working angular velocity of the blade considering contact friction is about  $1 \times 10^4$  rpm,  $1 \times 10^4 \sim 2 \times 10^4$  rpm and  $2 \times 10^4$  rpm, respectively. The first three order frequency curve intersects with the excitation frequency line  $K = 5$ ,  $K = 2$  and  $K = 8$ , respectively, and the resonance is easy to occur.

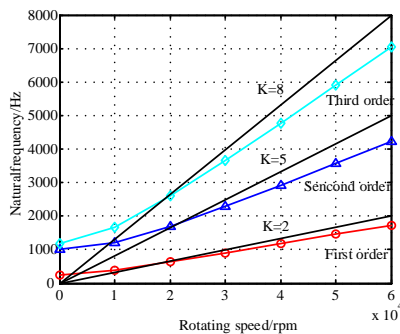


Fig.9 Campbell diagram of the blade with contact friction at the root

## CONCLUSIONS

Vibration and friction damping analysis of the blade between blade-root and disc-slot are researched. The effects of normal contact stiffness, normal contact damping of blade dovetail attachment, and rotating angular velocity on vibration response of blade are analyzed. The following results are drawn.

1) Blade considering contact friction characteristics simplified as a cantilever beam. Blade is subjected to uniform Pneumatic loads, centrifugal loads, and contact forces between the contact surface of blade dovetail attachment. The spring and viscous dampers are used to characterize the normal pressure in blade dovetail attachment, and the friction between the contact surface of blade dovetail attachment is characterized by the Coulomb friction model.

2) The influence of contact force on stiffness and damping matrix of the blade is introduced into the dynamical equation of a cantilever blade. The resonant response of blade is obtained by the Newmark method.

3) When the range of the normal stiffness of the contact area is within  $10^4\text{N/m}$  to  $10^8\text{N/m}$ , the amplitude of resonant response of blade decreases. When the normal contact stiffness is maintained at  $10^7\text{N/m}$  to  $10^8\text{N/m}$ , damping effect is obvious. The contact damping of the contact interface has little effect on the amplitude of the resonant response of the blade.

## ACKNOWLEDGMENT

This work is financially supported by National Natural Science Foundation of China (No.11502227), Shandong Provincial Natural Science Foundation, China (No. ZR2014EEP006) and the Tribology Science Fund of State Key Laboratory of Tribology(No. SKLTKF18B12).

## REFERENCES

- Afzal, M., Arteaga, L. I., Kari, L., "An analytical calculation of the Jacobian matrix for 3D friction contact model applied to turbine blade shroud contact,"; *Computers and Structure*, Vol.177, pp.204-217(2016).
- Afzal, M., Arteaga, I. L., Kari, L., "Numerical analysis of multiple friction contacts in bladed disks, *International Journal of Mechanical Sciences*,"; Vol.137, pp.224–237(2018).
- Araújo, J. A., Nowell, D., "Mixed high low fretting fatigue of Ti6Al4V: Test and modeling, *Tribology International*,"; Vol.42, pp. 1276-1285(2009).
- Botto, D., Lavella, M., "A numerical method to solve the normal and tangential contact problem of elastic bodies, *Wear*,"; Vol.330–331, pp. 629-635(2015).
- Chen, J. J., Menq, C.H., "Prediction of periodic response of blades having 3D nonlinear shroud constraints,"; *Journal of Engineering for Gas Turbines and Power*, Vol.123, No.4, pp.901-909(2001).
- Chen, J. J., Yang, B. D., Menq, C. H., "Periodic forced response of structures having three dimensional frictional constraints,"; *Journal of sound and vibration*, Vol. 229, No.4, pp.779-792(2000).
- Cui, Y., "Dynamic research of rigid-flexibly coupling system in stream turbine blades,"; Harbin Engineering University, Harbin, China(2008).
- DenHartog, J.P., "Forced vibrations with combined coulomb and viscous friction,"; *Transactions of the American Society of Mechanical Engineers*, Vol. 53, No. 1, pp.107-115(1931).
- Ferri, A. A., "Dowell E. H. Frequency domain solutions to multi-degree-of-freedom, dry friction damped systems,"; *Journal of Sound and Vibration*, Vol.124, No.2, pp. 207-224(1988).
- Fan, T.Y., "Vibration Reduction by Elastic Support Dry Friction Damper,"; Ph. D. Thesis, Northwestern Polytechnical University, Xi'an, China(2006).
- Gordon, C. K., "Forced vibration of a two degree of freedom system with combined coulomb and viscous damping,"; *Journal of Acoustical Society of America*, Vol. 39, No. 1, pp. 14-24(1966).
- Gu, Y. X., "Research on fretting fatigue life of dovetail joint under HCF-LCF load,"; Nanjing University of Aeronautics and Astronautics, Nanjing, China(2007).
- Hoffmann, T., Scheidta, L. P., Wallaschek J., "Modelling friction characteristics in turbine blade vibrations using a fourier series expansion of a real friction hysteresis, *Procedia Engineering*,"; X International Conference on Structural Dynamics, EURO DYN (2017).
- Krack, M., Salles, L., Thouverez, F., "Vibration prediction of bladed disks coupled by friction joints, *Archives of Computational Methods in Engineering*,"; Vol.24, pp. 589-636(2017).
- Kaya, M.O., "Free vibration analysis of a rotating Timoshenko beam by differential transform method,"; *Aircraft Engineering and Aerospace Technology*, Vol.78, No.3, pp.194-203(2006).
- Lassalle, M., Firrone, C.M., "A parametric study of Limit Cycle Oscillation of a bladed disk caused by flutter and friction at the blade root joints,"; *Journal of Fluids and Structures*, Vol.76, pp.349-366(2018).
- Muszynska, A., Dig, J., "Bladed disk dynamics investigated by a discrete model: effects of traveling wave excitation friction and mistuning,"; *Proceedings of the Machinery Vibration Monitoring and Analysis Meeting*, pp.33-49(1982).
- Pierre, C., Ferri, A. A., Dowell, E.H., "Multiharmonic analysis of dry friction damped systems using an incremental harmonic balance method,"; *Journal of Applied Mechanics*, Vol.52, No.4, pp. 958-964(1985).
- Papanikos, P., Meguid, S.A., "Theoretical and experimental studies of fretting-initiated fatigue failure of aeroengine compressor discs,"; *International Journal of Fatigue*, Vol.17, No.6, pp. 449-449(1995).
- Pesaresi, L., Salles, L., Jones, A., Green, J.S., et al, "Modelling the nonlinear behaviour of an underplatform damper test rig for turbine applications, *Mechanical Systems and Signal Processing*,"; Vol.85, pp.662–679 (2017).
- Rajasekaran, R., Nowell, D., "Fretting fatigue in dovetail blade roots: Experiment and analysis. *Tribology International*,"; Vol.39, No.10, pp. 1277-1285(2006).
- Sazhenkova, N., Semenovab, I., Nikhamkina, M., Semenova, S., "A substructure-based numerical technique and experimental analysis of turbine blades damping with underplatform friction dampers, *Procedia Engineering*,"; Vol.199, pp.820-825(2017).
- Tang, W. H., Epureanu, B. I., "Nonlinear dynamics of mistuned bladed disks with ring dampers,"; *International Journal of Non-Linear*

- Mechanics, Vol.97, pp.30-40(2017).
- Voldich, J., Polach, P., Lazara, J., "Use of Cyclic Symmetry Properties in Vibration Analysis of Bladed Disks with Friction Contacts between Blades,"; Procedia Engineering, Vol.96, pp.500-509(2014).
- Wen, M., "Research on characteristics and control methods of dry friction system,"; Northwestern Polytechnical University, Xi'an, China(2003).
- Wang, Z., "Research on fretting fatigue life reliability of dovetail joint,"; Nanjing University of Aeronautics and Astronautics, Nanjing, China(2008).
- Wang, J., "Research on Vibration Analysis Methods and Vibration Suppression Effect of Damping Structure of Blade,"; Ph. D. Thesis, School Of Mechanical Engineering and Automation, Northeastern University, Shenyang, China(2013).
- Xu, Z. L., Li, X. Y., Yuan, Q., "Analysis of Response of Blades with Friction Damping Interconnect or Using a New Friction Model,"; Journal of Xi'an Jiaotong University, Vol. 32, No.1, pp. 42-44(1998).
- Xia, Q. Y., "Research on fretting fatigue life of dovetail joint under low cycle load,"; Ph. D. Thesis, Nanjing University of Aeronautics and Astronautics, Nanjing, China(2005).
- Yang, B. D., Menq, C. H., "Characterization of contact kinematics and application to the design of wedge dampers in turbomachinery blading, Part 1 Stick-slip contact kinematics,"; Journal of Engineering for Gas Turbine and Power, Vol.120, No.2, pp. 410-417(1998).
- Yang, W. J., "Prediction method on fretting fatigue life of dovetail joint,"; Ph. D. Thesis, Nanjing University of Aeronautics and Astronautics, Nanjing, China(2007).
- Zhang, J., Liu, X. P., "Theoretical and numerical methods for vibration modal analysis of Turbomachinery,"; National Defense Industry Press, Beijing, China(2001).

## NOMENCLATURE

- $\Omega$  Rotational angular velocity  
 $R$  Distance  
 $\rho$  Density  
 $E$  Elastic modulus  
 $\nu$  Poisson's ratio  
 $L_0$  Length  
 $B$  Width  
 $H$  Thickness  
 $A$  Cross-sectional area  
 $F_a(t)$  Pneumatic load  
 $F_N$  Positive pressure

- $F_f$  Friction force  
 $f(x)$  Axial centrifugal load  
 $M(x,t)$  Bending moment  
 $Q(x,t)$  Shear force  
 $M$  Mass matrix  
 $K$  Stiffness matrix of the blade  
 $C_{con}$  Contact damping matrix  
 $K_e$  Elastic stiffness matrix centrifugal  
 $K_c$  Centrifugal stiffness matrix  
 $K_{con}$  Contact stiffness matrix

## 考慮葉根摩擦阻尼的葉片的動力學分析

王嬌 於濤 張曰浩  
 煙臺大學機電汽車工程學院

韓清凱  
 大連理工大學機械工程學院  
 摘要

本文提出一種研究葉根接觸面間的摩擦阻尼和接觸特性對葉片動力學特性影響的理論方法。首先建立了葉片葉根榫頭-榫槽的簡化力學模型，模型由質量、彈簧和阻尼器構成，阻尼器摩擦力採用宏滑移摩擦模型，推導出接觸摩擦的數學運算式。然後，建立了離心力作用下考慮葉根摩擦阻尼的葉片的運動方程，考慮了分佈週期氣動載荷和內部阻尼。使用伽遼金法獲得了三自由度接觸摩擦模型。最後，採用數值法對接觸摩擦模型進行了強迫振動響應分析。研究葉根榫頭-榫槽之間的接觸剛度和接觸阻尼，葉片轉速對葉片動力學特性的影響規律。結果表明，葉根摩擦阻尼可以降低葉片的振動幅值，當接觸剛度在  $10^7$  N/m 到  $10^8$  N/m 的範圍內，減振效果較好。